

MAGNETOSPHERIC GAP AND ACCUMULATION OF GIANT PLANETS CLOSE TO THE STAR

M.M. ROMANOVA

Department of Astronomy, Cornell University, Ithaca, NY 14853-6801; romanova@astro.cornell.edu

R.V.E. LOVELACE

Departments of Astronomy and Applied Physics, Cornell University, Ithaca, NY 14853-6801; RVL1@cornell.edu

Subject headings: accretion, dipole — plasmas — magnetic fields — stars: magnetic fields — X-rays: stars

Draft version February 5, 2008

ABSTRACT

The bunching of giant planets at a distance of several stellar radii may be explained by the disruption of the inner part of the disk by the magnetosphere of the star during the T Tauri stage of evolution. The rotating magnetic field of the star gives rise to a low density magnetospheric gap where stellar migration is strongly suppressed. We performed full 3D magnetohydrodynamic simulations of the disk-magnetosphere interaction and examined conditions for which the magnetospheric gap is “empty”, by changing the misalignment angle between magnetic and rotational axes of the star, Θ , and by lowering the adiabatic index γ , which mocks up the effect of heat conductivity and cooling. Our simulations show that for a wide range of plausible conditions the gap is essentially empty. However, in the case of large misalignment angles Θ , part of the funnel stream is located in the equatorial plane and the gap is not empty. Furthermore, if the adiabatic index is small ($\gamma \sim 1.1$) and the rotational and magnetic axes are almost aligned, then matter penetrates through the magnetosphere due to 3D instabilities forming high-density equatorial funnels. For these two limits there is appreciable matter density in the equatorial plane of the disk so that a planet may migrate into the star.

1. INTRODUCTION

More than 170 giant planets have been discovered around solar-type stars (see catalog of planets in <http://vo.obspm.fr/exoplanetes/encyclo/catalog-main.php>). About 24% of them are located very close to the star, at $r \lesssim 0.1\text{AU}$ (see also reviews by Marcy et al. 2003; Papaloizou & Terquem 2006). There is a prominent peak in the radial distribution of the planets at $r \sim 0.04 - 0.05 \text{ AU} \approx (7 - 10)R_{\odot}$ which corresponds to periods of 3 days (see Figure 1).

The radial distribution and other properties of the giant planets have stimulated work on models of planet formation and migration. According to the presently favored interpretation, planets form far away from the star either through core accretion (Mizuno 1980; Pollack et al. 1996), or through instabilities in the disk (Boss 2001). Subsequently they migrate inward due to their gravitational interaction with the disk (Lin & Papaloizou 1986; Lin, Bodenheimer & Richardson 1996; Ward 1997; Nelson & Papaloizou 2003).

Some planets may migrate close to the star where the disk properties are strongly influenced by the star and/or the star’s magnetic field. In particular, the inner regions of the disk may be truncated as a result of heating by the star (e.g., Kuchner & Lecar 2002) and photoevaporation of the region of the disk $\lesssim 1 \text{ AU}$ (Matsuyama, Johnstone & Murray 2003). Or, the inner part of the disk may be disrupted by the strong magnetic field of the protostar (Lin et al. 1996).

There are strong observational arguments that young solar-type stars (T Tauri type stars) have strong magnetic fields. They are thousands of times brighter than the Sun

in the X-ray (see review by Feigelson & Montmerle 1999) which is a sign of their high magnetic activity. In a number of cases, direct measurements of the Zeeman broadening imply a B field (averaged over the surface of the star) of the order of several kilo-Gauss, which is much stronger than that the average field on the surface of the Sun (e.g., Basri et al. 1992; Johns-Krull et al. 1999). The strongest magnetic fields are probably associated with the multipolar component (e.g. Safer 1998; Johns-Krull et al. 1999; Smirnov et al. 2003). However, a significant dipole component is also expected. It gives many observational signs of magnetospheric accretion in the T Tauri stage (see review by Bouvier et al. 2006) and also is observed in some circular polarization measurements (e.g., Valenti & Johns-Krull 2004; Symington et al. 2005).

A sufficiently strong dipole magnetic field will truncate the disk at a distance of several stellar radii forming a low-density magnetospheric gap as shown in Figure 2. The migration rate of planets in this gap will be greatly reduced.

This work analyzes the conditions where a low-density gap exists between the inner edge of the disk and the star’s surface. Our analysis is based on 3D MHD simulations. In particular, we investigate properties of the gaps for different misalignment angles Θ between the rotation axis of the star Ω_* and its magnetic moment μ . We investigate conditions where part of the funnel stream is in the equatorial plane close to the star. This may give an appreciable matter density in the magnetospheric gap. Also we consider the possibility of direct equatorial accretion from the disk to the star due to 3D instabilities.

2. WHERE DOES THE PLANET MIGRATION STOP?

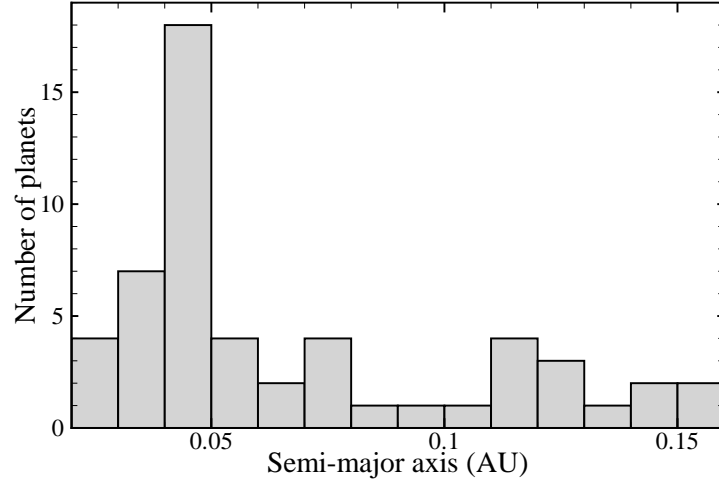


FIG. 1.— Distribution of extrasolar planets in the vicinity of the star.

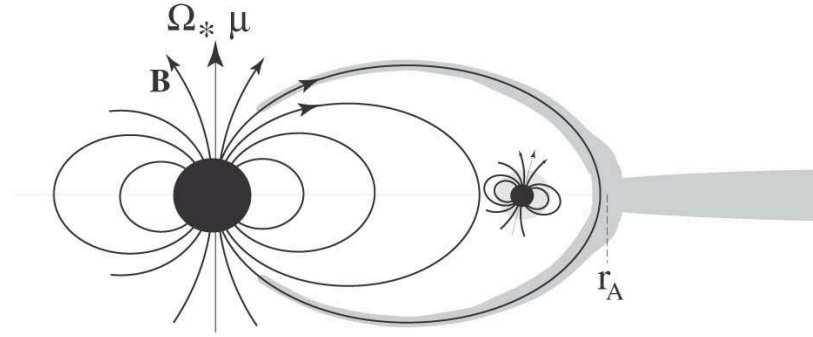


FIG. 2.— Sketch of an accretion disk which is disrupted by the star's dipole magnetic field. The rate of migration of a planet is greatly slowed once it enters the gap.

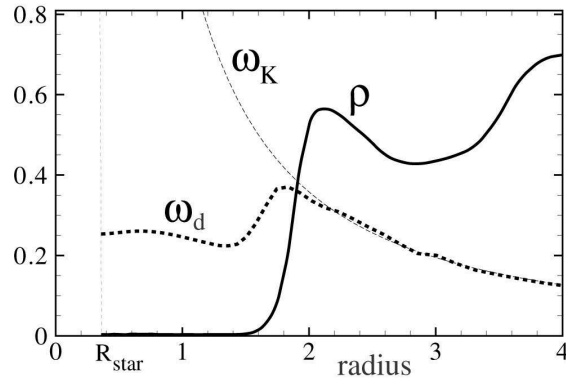


FIG. 3.— Radial distribution of the density (solid line) and the angular velocity of the disk $\omega_d = v_\phi/r$ (dashed line) in the vicinity of the star for a misalignment angle of $\Theta = 30^\circ$. Thin dashed line shows Keplerian angular velocity ω_K .

The accretion disk is disrupted at the Alfvén radius where the dynamic pressure of the disk matter is comparable to the magnetic pressure in the star's dipole field,

$$r_A = [\mu^2 / (\dot{M} \sqrt{GM})]^{2/7} \text{ or } r_A \approx 7.2 \times 10^{11} \frac{B_3^{4/7} R_{2.5}^{12/7}}{M_{0.8}^{1/7} \dot{M}_{-7}^{2/7}} \text{ cm} \approx 0.05 \text{ AU}, \quad (1)$$

where $M_{0.8} \equiv M_*/0.8M_\odot$, $R_{2.5} \equiv R_*/2.5 R_\odot$, and $B_3 \equiv B_*/10^3 \text{ G}$ are the normalized mass, radius, and magnetic

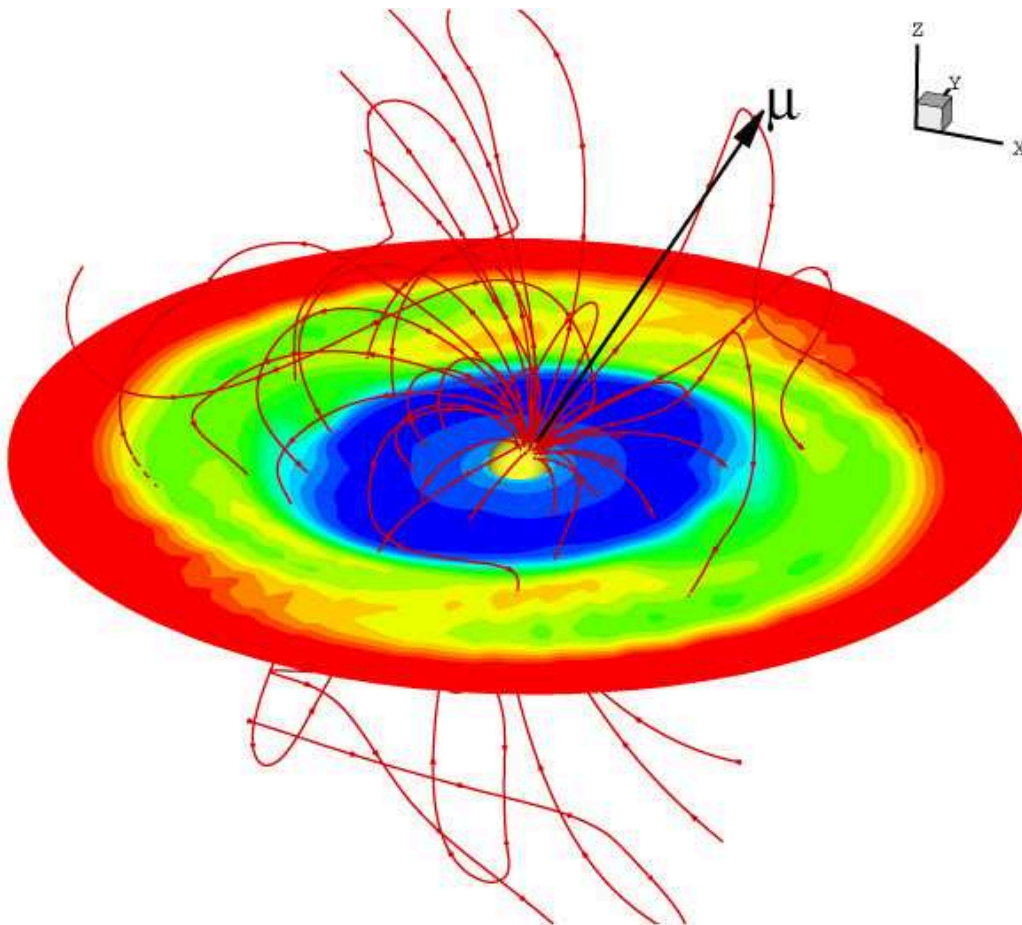


FIG. 4.— Result of 3D simulations of disk accretion to a rotating star with a dipole moment μ misaligned with the star's rotation axis Ω_* by $\Theta = 30^\circ$. The color background shows the density distribution in the equatorial region. Density varies from $\rho \approx 0.003$ (blue color) to $\rho \approx 1$ (red color). The red lines are magnetic field lines. The black arrow shows the direction of the magnetic moment μ .

field of the protostar, and $\dot{M}_{-7} \equiv \dot{M}/10^{-7} M_\odot/\text{yr}$ is the accretion rate in the disk (Ghosh & Lamb 1979; Camenzind 1990; Königl 1991). For the typical parameters of T Tauri stars used in this formula, this radius coincides approximately with the peak of the distribution shown at Figure 1. Thus this peak may result from the greatly reduced rate of migration inside the magnetospheric gap.

Numerical simulations show that the disk is disrupted at the distance $r \approx r_A$, where the plasma is lifted out of the disk plane by the vertical pressure force and it then flows along the star's dipole field lines in a funnel flow (Romanova et al. 2002; 2003; 2004). As a consequence, the density of matter in the equatorial plane is greatly reduced for $r < r_A$. Figure 3 shows the equatorial density distribution obtained from our 3D simulations. The density is large in the disk, and it often increases as r_A is approached. However, for $r < r_A$ the density drops by a factor of $\sim 100 - 300$ in the magnetically-dominated magnetosphere. A protoplanet which migrates inward to radii $< r_A$ enters a region of greatly reduced density.

For typical conditions planets migrate inward as a result of interaction of the planet with the disk matter. The planet loses part of its orbital angular momentum by overtaking collisions with the disk outside its orbit and it gains

a smaller part by overtaking collisions of the disk matter inside its orbit. The rate of migration, or radial speed, V_{pr} , depends on a number of parameters such as mass of the planet, M_p , surface density of the disk, Σ , viscosity in the disk, ν , and others, and also it is different in cases when a planet opens a gap in the disk or not.

If the planet's mass is relatively small ($M_p \lesssim 10M_\oplus$) it does not open a gap in the accretion disk. The migration in this case is referred to as “type I,” and the planet's inward drift speed is $V_{pr} \propto -M_p(\Sigma r^2)$ (Ward 1997; Papaloizou & Terquem 2006).

Planets of sufficiently large mass open a gap in the disk of width of the order of the disk thickness. The migration in this case is referred to as “type II,” and it tends to “lock” the planet's migration to that of the disk matter if the local disk mass, $M_d = 4\pi r^2 \Sigma$, is larger than the planet's mass M_p . The disk matter moves inward with a radial speed $v_r = -3\nu/(2r)$, where $\nu = \alpha c_s^2/\omega_K$ is the usual Shakura-Sunyaev turbulent viscosity with $\alpha = 10^{-3} - 10^{-2}$. However, if the local disk mass is small compared with the planet's mass, then the planet's migration is slower than that of the disk matter. The angular momentum lost by the planet $dJ_p/dt = M_p v_K V_{pr}/2$ in a second is equal to the angular momentum transported outward by the vis-

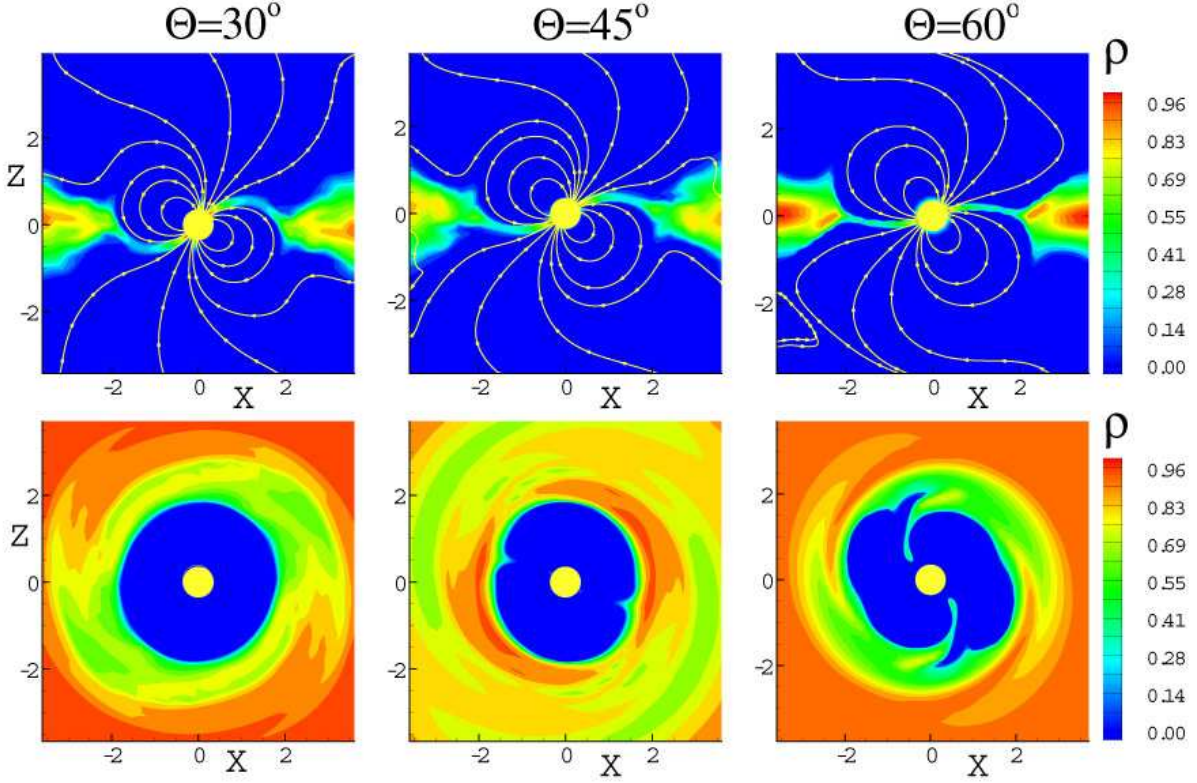


FIG. 5.— The top panels show the density distributions and sample magnetic field lines in the $\Omega_* - \mu$ plane for different misalignment angles $\Theta = 30^\circ, 45^\circ, 60^\circ$. The bottom panels show the equatorial distribution of density.

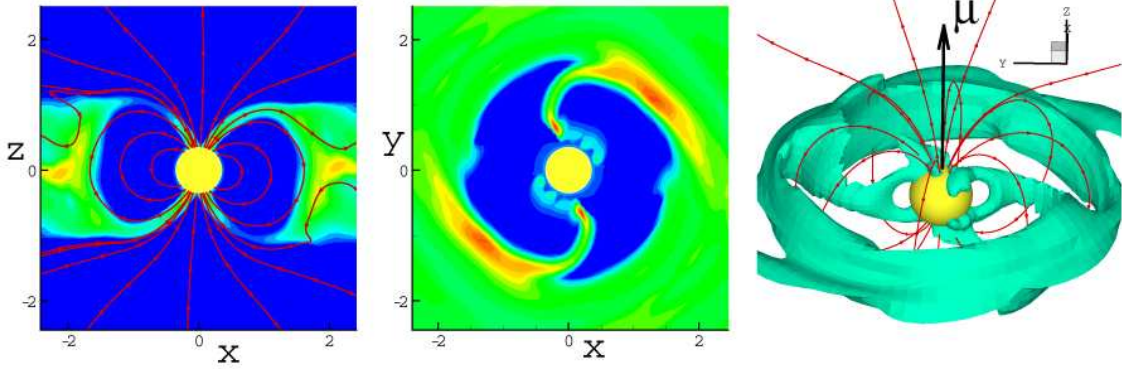


FIG. 6.— Result of simulations for $\gamma = 1.1$ for $\Theta = 5^\circ$ after $P = 12$ rotations. The left panel shows the density distribution and sample field lines in the $\Omega_* - \mu$ plane. The middle panel shows the density distribution in the equatorial plane, and the right panel shows a 3D view of the density levels and sample field lines.

cous stress in the disk, $dJ_d/dt = \dot{M}rv_K$, where $v_K = (GM/r)^{1/2}$ is the Keplerian velocity and \dot{M} mass accretion rate of the disk. This gives a migration speed of the planet $V_{pr} = -(M_d/M_p)|v_r|$. We can write $\dot{M} = 2\pi r\Sigma|v_r|$ so that $M_d = 4\pi r^2\Sigma \approx 1.3 \times 10^{29} g(r/0.1\text{AU})^{3/2} (\dot{M}/10^{-7}M_\odot/\text{yr})$ for $h/r = 0.1$ and $\alpha = 10^{-3}$.

For $M_d < M_p$, the time scale for the planet's migration at r is simply

$$\tau_p = \frac{r}{V_{pr}} = \frac{M_p}{M_d} \frac{2r^2}{3\nu}, \quad (2)$$

which is independent of r and inversely proportional

to both \dot{M} and α . For a Jupiter mass planet, $\tau_p \approx 4700\text{yr}(10^{-7}M_\odot/\text{yr}/\dot{M})$ for $\alpha = 10^{-3}$ and $h/r = 0.1$. However, equation(2) does not include the influence of the star's magnetic field. Inside the magnetospheric gap the matter density is reduced by a factor $\gtrsim 10^2$. The migration time will be increased by a corresponding factor.

Figure 3 also shows that the angular velocity of the disk plasma in the equatorial plane ω_d within the magnetospheric gap is much lower than the Keplerian angular velocity of the planet ω_K for stars with periods $P \gtrsim 2$ days. Thus, the disk matter passing close by the planet will have a large relative velocity $r(\omega_K - \omega_d)$. The relative veloc-

ity is larger than in the non-magnetic case by a factor $F \sim (r/h)(\omega_K - \omega_d)/\omega_K \gg 1$ for the type II migration. One can readily show that the rate of exchange of angular momentum between the planet and the disk is reduced by a factor $1/F^2 \ll 1$. Thus the migration time inside the magnetospheric gap will be increased further by a factor F^2 . We estimate $F^2 \gtrsim 10$. Once the planet is inside the magnetospheric gap it may continue to migrate slowly inward owing to resonances it has with the disk matter at larger radii but a treatment of this is beyond the scope of the present work.

Thus, in both cases the migration will be greatly reduced if the density in magnetospheric gap is much lower than in the disk. Conditions may be changed however if the magnetic axis μ is misaligned relative to the rotational axis of the star Ω_* by an angle Θ . For high misalignment angles Θ , the funnel streams may be partially located in the equatorial region (Romanova et al. 2003). From the other side, even in the aligned case, some matter may accrete to the star in the equatorial plane due to instabilities (e.g., Arons & Lea 1976). We performed 3D simulations to investigate both factors.

3. 3D SIMULATIONS OF THE DISK-MAGNETOSPHERE INTERACTION AND MAGNETOSPHERIC GAPS

We performed a set of 3D simulations using our code based on the “cubed sphere” grid (Koldoba et al. 2002) with the main goal of analyzing the density distribution in the magnetospheric gap. Simulations were set up in a way similar to those of Romanova et al. (2003, 2004). Namely, quasi-stationary initial conditions were used which permitted slow viscous accretion from the disk to a star. An α -viscosity was incorporated to the code with typical values of α -parameter: $\alpha = 0.02$ and 0.04 . The magnetic axis μ is misaligned relative to rotational axis of the star Ω_* by an angle Θ . The rotational axis of the star coincides with that of the disk.

Simulations were done for parameters typical for T Tauri type stars: $M_* = 0.8M_\odot$, $R_* = 2.5R_\odot$, $B_* = 10^3 G$, $\dot{M} \approx 3 \times 10^{-8} M_\odot/\text{yr}$. Compared to our previous 3D runs, we changed parameters so as to increase the size of magnetospheric gap to $r_A = (4 - 5)R_*$ versus $r_A = (2 - 3)R_*$ in our previous papers. Figure 4 shows the magnetospheric gap in a test case with an even larger magnetosphere $r_A = (6 - 7)R_*$. One can see that the low-density magnetospheric gap can be quite large. One can also see that inside the magnetospheric radius (which corresponds approximately to the edge of the disk), the magnetic field lines are closed, while outside of this radius they are carried by the matter of the disk or corona. Our simulations show that the density inside the magnetospheric gap is about 100 – 300 times smaller than the density in the nearby disk.

Magnetospheric Gap at Different Θ . We performed 3D simulations for different misalignment angles Θ from $\Theta = 0^\circ$ to 90° . We investigated the magnetospheric gaps in the equatorial plane. Simulations have shown that matter flow is different at small and large misalignment angles. For angles $\Theta \lesssim 45^\circ$, matter flows to the star along funnel streams which are above and below the equatorial plane. Thus within the magnetospheric gap $r < r_A$ the matter density in the equatorial plane is greatly reduced

(see Figure 5, left two panels). For larger angles, matter also accretes to a star through the funnel streams. However, part of the funnel streams is located in the equatorial plane and the magnetospheric gap is not empty (Figure 5, right panel). Thus at large Θ , the planets orbiting in the equatorial plane will interact with the dense gas of the streams and may continue to migrate inward to the star.

Accretion through Equatorial Funnels at Low γ . There is another possible reason why the magnetospheric gap may have some matter density. There are possible instabilities which may lead to the direct accretion of matter through the magnetosphere in the equatorial plane. To investigate such instabilities, we took the almost aligned case, $\Theta = 5^\circ$, and decreased the adiabatic index from $\gamma = 5/3$ to $\gamma = 1.1$. The adiabatic index may be significantly lower than its ideal value in the case of high electron heat conductivity which may occur in a highly ionized plasma. In our simulations, the low value of γ acts to give a low temperature in the disk and the funnel flow. We observed that matter partially accretes in the equatorial plane. Figure 6 shows that matter accreted through funnels which are located inside the magnetosphere. They penetrate inwards through the Rayleigh-Taylor type instability (e.g. Arons & Lea 1976) up to some distance r_1 , and then form regular funnel streams along the field lines. The distance of penetration depends on the ratio r_A/R_* . At relatively small values r_A/R_* , the equatorial funnels may penetrate almost to the surface of the star, as shown in Figure 6. At larger values of r_A/R_* , the funnels move inward only part of the way. Thus, in the case of a weak magnetic field and/or high accretion rate, the magnetospheric radius $r_A \approx (1 - 3)R_*$, and a small adiabatic indexes γ , the gap will not be empty and planets will continue to migrate inward unless the tidal interaction or some other force will prevent them against falling to the star. In the opposite case of a larger magnetosphere, the equatorial funnels will occupy only a part of the gap and planet may survive longer inside the innermost gap.

4. CONCLUSIONS

We conclude that for typical parameters of solar-type protostars a very low-density magnetospheric gap forms. We show that the rate of inward migration of protoplanets is greatly reduced within this gap. This gap may explain the observed accumulation of planets at the distances $\sim (0.04 - 0.05)$ AU from the star. Note however that there may be significant matter density within r_A in cases of high misalignment angles $\Theta \gtrsim 45^\circ$ where the part of the funnel stream is located in the equatorial plane. Further, for low values of the adiabatic index, $\gamma = 1.1$, and small misalignment angles, $\Theta \lesssim 5^\circ$, matter may accrete in the equatorial plane due to instabilities. However, the azimuthal velocity of the matter within r_A differs substantially from the Keplerian angular velocity of the planet. This difference in the velocities acts to slow the planet’s migration.

We thank Drs. G.V. Ustyugova and A.V. Koldoba for valuable contributions to our MHD simulation codes. Also we thank the referee for thoughtful comments. This work was supported in part by NASA grant NNG05GL49G and by NSF grant AST-0507760.

REFERENCES

- Arons, J. & Lea, S.M. 1976, *ApJ*, 207, 914
 Basri, G., Marcy, G.W., & Valenti, J.A. 1992, *ApJ*, 390, 622
 Boss, A.P. 2001, *ApJ*, 563, 367
 Bouvier, J., Alencar, S., Harries, T.J., Johns-Krull, C.M., & Romanova, M.M. 2006, *Protostars and Planets V*, accepted
 Camenzind, M. 1990, *Rev. Modern Astron.*, 3, 234
 Feigelson, E.D., & Montmerle, T. 1999, *Ann. Rev. Astron. Astrophys.*, 37, 363
 Ghosh, P., & Lamb, F.K. 1979, *ApJ*, 234, 296
 Johns-Krull, C., Valenti, J.A., & Koresko, C. 1999, *ApJ*, 516, 900
 Koldoba, A.V., Romanova, M.M., Ustyugova, G.V., & Lovelace, R.V.E. 2002, *ApJ*, 576, L53
 Königl, A. 1991, *ApJ*, 370, L39
 Kuchner, M.J., & Lecar, M. 2002, *ApJ*, 574, L87
 Lin, D.N.C., Bodenheimer, P., & Richardson, D.C. 1996, *Nature*, 380, 606
 Lin, D.N.C., & Papaloizou, J. 1986, *ApJ*, 309, 846
 Marcy, G.W., Butler, R.P., Fischer, D.A., & Vogt, S.S. 2003, *Scientific Frontiers in Research on Extrasolar Planets*, ASP Conference Series, Vol. 294, Eds. Deming, D. & Seager, S.
 Matsuyama, I., Johnstone, D., & Murray, N. 2003, *ApJ*, 585, L143
 Mizuno, H. 1980, *Prog. Theor. Phys.*, 64, 544
 Nelson, R.P., & Papaloizou, J.C.B. 2003, *MNRAS*, 339, 993
 Papaloizou, J.C.B., & Terquem, C. 2006, *Rep. Prog. Phys.*, 69, 119
 Pollack, J.B., Hubickyj, O., Bodenheimer, P., et al. 1996, *Icarus*, 124, 62
 Romanova, M.M., Ustyugova, G.V., Koldoba, A.V., & Lovelace, R.V.E. 2002, *ApJ*, 578, 420
 Romanova, M.M., Ustyugova, G.V., Koldoba, A.V., Wick, J.V., & Lovelace, R.V.E. 2003, *ApJ*, 595, 1009
 Romanova, M.M., Ustyugova, G.V., Koldoba, A.V., & Lovelace, R.V.E. 2004, *ApJ*, 610, 920
 Safier, P.N. 1998, *ApJ*, 494, 336
 Smirnov, D.A., Lamzin, S.A., Fabrika, S.N., & Valyavin, G.G. 2003, *A&A*, 401, 1057
 Symington, N.U., Harries, T.J., Kurosawa, R., & Naylor, T. 2005, *MNRAS*, 358, 977
 Valenti, J.A. & Johns-Krull, C. 2004, *Astrophys. Sp. Sci. Ser.*, 292, 619
 Ward, W.R. 1997, *ApJ*, 482, L211